

EXPERIMENTAL RESULTS ON THE COMBINED 1ST AND 2ND ORDER DYNAMICS OF A SMALL-SCALE TAUT-LEG MOORING LINE

Alexandre N. Simos
Naval Arch. & Ocean Eng. Dept.
University of São Paulo

André L. C. Fuarra
Naval Arch. & Ocean Eng. Dept.
University of São Paulo

Fábio G. Palazzo
CENPES/Petrobras

ABSTRACT

A set of experimental results on the dynamics of taut-leg mooring-lines was generated by means of towing-tank tests. These results will be employed by Petrobras as an experimental paradigm for the calibration and validation of numerical codes based on finite-elements method (FEM). The setup allowed combining first and second order motions on the top of the line with different amplitudes and frequencies. The first order motions were emulated by means of circular harmonic motions while alternate horizontal translations represented the drift motions. It was also possible to emulate a uniform in-plane current profile along the suspended length of the model.

The model was composed by three different segments. An intermediate rubber hawser connected the top and anchor chain segments and allowed considerable elongation of the line during the tests. Tension at the top of the model was measured by means of a load cell and the second-order motion was registered optically.

This paper presents the procedure adopted for the tests and also some preliminary comparisons between experimental results and numerical simulations.

Keywords: Taut-leg mooring, towing-tank tests, combined motions, dynamic tension

INTRODUCTION

Among the many challenges imposed by deep-water oil production, the research and development of suitable mooring systems has deserved a great effort in recent years. As depth increases, the transition from heavy all-steel catenary mooring systems to lighter taut-leg chain moorings – fiber rope combinations allows for reduced offsets, increased payloads and reduced sea floor footprints. One of the main issues concerning

the R&D of deep-water mooring systems is the choice for the best material for specific applications. High Efficiency Polyester and Nylon represent two of the most usual choices. Over the past few years the topic has been included in many joint industry projects and a good number of papers dedicated to the development and analysis of lightweight fiber ropes for deep-water mooring systems can be found in literature (see, for instance, [1], [4] and [7]).

As one of the leaders in deep-water technology, Petrobras faces the challenge of making offshore production feasible to water depths over 3000 meters. For an estimated production of 1.9 million bopd in 2006, 70% of the total production will come from deep or ultra-deep-waters offshore Campos Basin. Since 2000, Petrobras has conducted strategic R&D projects (Procap 2000 and Procap 3000) with the cooperation of major Brazilian universities to cope with the future requirements for ultra-deep-water production and the development of reliable, cost-effective mooring systems is one of the key issues.

Although taut-leg chain-fiber moorings are nowadays a reality for the most recent systems offshore Campos Basin for water depths up to around 1000 m, these configurations still pose many challenges to the designer. Apart from the aforementioned problem of material choices, the analysis of the system dynamics has to deal with the highly non-linear and time-dependent behavior of the composite materials, which influences the floating system seakeeping characteristics in an interactive way.

Due to the inherent complexity of the problem, it is not unusual that different numerical codes, usually based on FEM, provide somewhat discrepant results when dealing with the dynamics of real deep-water moorings subjected to the top motions imposed by the floating system combined with ocean current effects. Therefore, in face of the increasing number of

commercial packages aimed for the numerical analysis of risers and mooring lines, Petrobras and the University of São Paulo (USP) developed a project for generating a basic experimental paradigm concerning the dynamic behavior of taut-leg and catenary mooring lines. Results should emulate the effects of top displacements imposed by the 1st and 2nd order motions of the floating unit combined with current action.

Since 2001, a series of towing tank tests with rigid and flexible risers and catenary mooring lines had already been performed at the State of São Paulo Research Institute (IPT) for the validation of the USP Numerical Offshore Tank. A summary of the results have been presented in [2], [5] and [6]. For the new series of tests the previous experimental setup was used but a new mechanism had to be built to combine circular (1st order) motions in the vertical plane and low-frequency horizontal (2nd order) motions. There was also the problem of emulating the taut-leg behavior subjected to considerable elongation of the model whilst preventing rupture of the model or excessive loads on the top load-cell. The solution adopted was to use an intermediate rubber segment with sufficiently low axial stiffness.

This paper describes the experimental procedure adopted for the tests with the model in taut-leg configuration. The setup and model characteristics are presented together with some illustrative results. A preliminary comparison with numerical simulations is presented based on the results provided by the software *Orcastex*®. Although not extensive, this comparison aims to discuss the overall aspects involved in the numerical reproduction of the experimental data. The analysis of the catenary configuration tests is under development and will be presented in a future paper.

NOMENCLATURE

- R mean top-anchor horizontal distance (Neutral pos.)
- h height of top-end mean position above waterline;
- H water depth;
- U towing (current) velocity;
- A₁ amplitude of circular (1st order) top-end motion;
- A₂ amplitude of alternate horizontal (2nd order) motion;
- f₁ frequency of 1st order motion;
- f₂ frequency of 2nd order motion;
- De external diameter;
- m mass per unit length in air;
- EA axial stiffness;
- EJ bending stiffness;
- Cd hydrodynamic drag coefficient;
- Cf friction coefficient;
- Cm added mass coefficient;
- A,B,d chain link dimensions (see Fig.5)

THE EXPERIMENTAL SETUP

All the tests were conducted at the IPT facilities. The towing tank is 240m long, 6m wide and 4m deep. Towing tests with submerged cables are performed with a submerged

platform, which is connected to the carriage and supports the model's anchor. The top of the model is connected to a mechanical device that performs the prescribed 1st order and drift motions. The whole apparatus is towed along the tank emulating a uniform in-plane current profile along the suspended length of the model. Fig.1 illustrates the experimental setup.

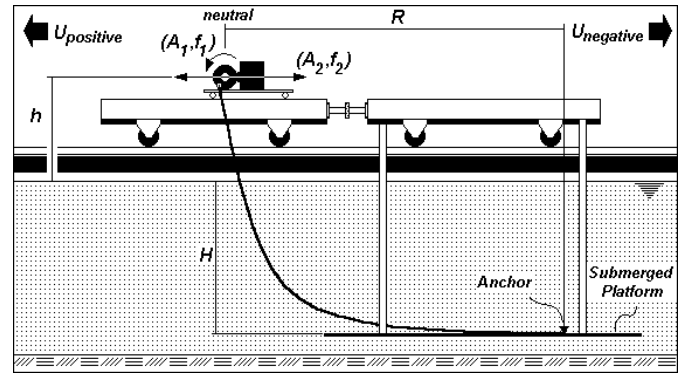


Fig.1 Experimental setup

For all the tests, H=3.02m and h=0.33m.

During the tests, tension at the top-end of the model is acquired by means of a load-cell. A pin connection between the load-cell and the rotating device guarantees that the top-end of the model is free to rotate. Top-end connection scheme is presented in Fig.2.

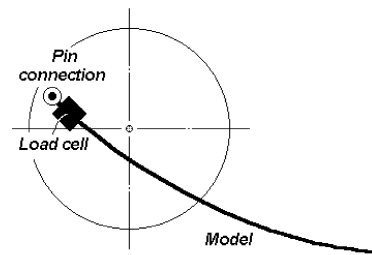


Fig.2 Top-end connection

The horizontal offset (2nd order motion) is monitored by means of an optical device.

TESTS PARAMETERS

It must be emphasized that the definition of tests parameters did not pursue any prescribed geometric resemblance with real-scale taut-leg mooring lines. Due to the physical constraints of the towing-tank facilities, it is almost impossible to guarantee geometrical and structural similarity with real deep-water mooring lines and still obtain a set of experimental results adequate for numerical validation purposes. Nevertheless, when defining the tests parameters some qualitative aspects of real-scale problems were followed, whenever it was possible.

The horizontal offset $A_2=0.30\text{m}$ was defined as 10% of the water-depth, a somewhat typical figure for deep-water moored systems. The ratio of 1st and 2nd order frequencies of motion was kept within the range $24 < f_1/f_2 < 120$.

Bearing in mind the numerical validation purposes, the choice of 1st order amplitudes and frequencies was made in order to guarantee that very different ratios between dynamic and static tensions would be achieved. The goal was to generate results with different levels of difficulty concerning their reproduction by numerical codes.

The mean horizontal distance between top and anchor ($R=7.00\text{m}$) was defined in a sense that the whole length of the model would be suspended in the so-called *Neutral* configuration, but the vertical load on the anchor would remain negligible.

Table 1 presents a summary of the parameters adopted in the tests. By combing these parameters, a total of 147 tests were performed.

Table 1 – Tests Parameters

R (m)	7.00
A_1 (m)	{0; 0.05; 0.10}
f_1 (Hz)	{0; 0.40; 0.55; 0.70; 0.85; 1.00}
A_2 (m)	{0; 0.30}
f_2 (Hz)	{1/120; 1/80; 1/60}
U (m/s)*	{0; +0.25; -0.25}

* The sign of U is defined according to Fig.1

THE MODEL

The model consisted of two chain segments connected by means of a rubber hawser with circular profile. Fig.3 presents a detail of the chain-rubber connection. As the top moves from *Neutral* to *Far* position, the intermediate rubber segment had to provide the necessary line elongation and at the same time guarantee structural integrity.

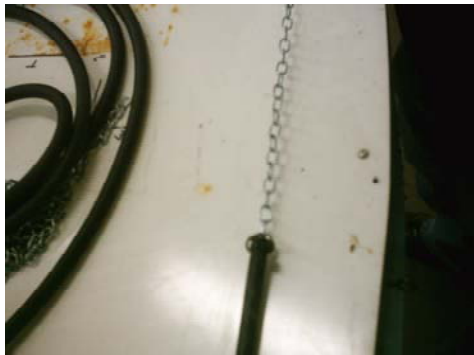


Fig.3 Detail of the model showing rubber-chain connection

Choosing a rubber profile with an adequate axial stiffness was then important in order to maintain the dynamic to static tension ratio between reasonable values. A set of preliminary numerical studies was carried out to help choosing an

appropriate axial stiffness and also to define a suitable load cell for top-end tension measurements.

The axial stiffness of the rubber profile was determined experimentally in a set of tension tests performed with five different specimens (S1 to S5). Load x Elongation curves are shown in Fig.4.

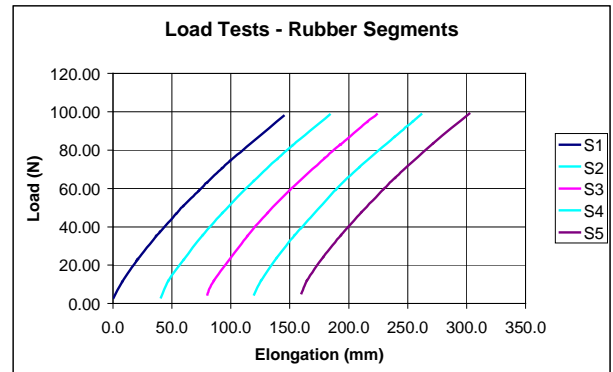


Fig.4 Load x Elongation curves obtained in tension tests

Mean value of Young Modulus is $E = 5.813 \text{ MPa}$ (with a standard deviation of 6%). Mean value of the axial stiffness was then assumed $EA = 0.759 \text{ kN}$.

Table 2 presents the model main dimensions. Properties for each segment are presented in Table 3.

Table 2 – Model Main Dimensions

Segment	Position	Type	Length
1	top	chain	1.00 m
2	intermediate	rubber	3.86 m
3	anchor	chain	3.00 m
Total length of the model			7.86 m

Table 3 – Segments Properties

		Chain	Rubber
External Diameter (De)		—	12.89 mm
Link dim.*	A	9.0 mm	—
	B	16.0 mm	—
	d	2.0 mm	—
Mass per length (m)		0.068 kg/m	0.173 kg/m
Axial stiffness (EA)		1320 kN	0.759 kN
Bending stiffness (EJ)		0	$7.88\text{E-}3 \text{ Nm}^2$

* chain link dimensions are defined respective to Fig. 5

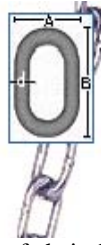


Fig.5 Definition of chain-link dimensions

EXPERIMENTAL RESULTS

A first set of experimental results was derived for some representative static configurations of the model. Static tension and angle¹ at the top were measured for three different static offsets. The first one was represented by the so-called *Neutral* configuration, defined by $R=7.00\text{m}$. *Near* and *Far* configurations were then obtained by imposing the maximum 2nd order offset $A_2=0.30\text{m}$ from the initial *Neutral* position of the top (hence, $R=6.70\text{m}$ and $R=7.30\text{m}$ for *Near* and *Far* situations, respectively). Tension and angle were measured for the zero-current condition ($U=0$) and also for $U=\pm 0.25\text{m/s}$. Static results are summarized in Table 4. They help to verify the consistency of numerical models prior to time-consuming dynamic analysis.

Table 4 – Static Values of Tension and Angle at the Top

Static Configuration:		Near	Neutral	Far
U (m/s) 0	Tension (N)	3.85	6.50	38.03
	Angle (°)	37	50	61
U (m/s) +0.25	Tension (N)	2.73	5.27	37.02
	Angle (°)	42	51	62
U (m/s) -0.25	Tension (N)	4.82	7.72	40.25
	Angle (°)	35	48	60

A second group of tests were then performed incorporating drift motions only ($A_1=0$; $A_2=0.30\text{m}$) for the three different values of 2nd order frequencies, with and without current effects. As an example, Fig.6 presents the results obtained for $f_2=1/60\text{Hz}$. The upper curve represents the second-order static excursion (offsets), expressed in centimeters. The lower curve brings the tension measured at the top of the model. Every test was performed for at least two complete cycles of the drift motion, which in this case corresponds to 120 seconds of acquisition. The drift-only results allows for calibration of the numerical model concerning the horizontal excursion of the top. It also provides a second check for the line axial stiffness since the model undergoes a significant amount of elongation as its top-end moves from the *Neutral* to the *Far* position.

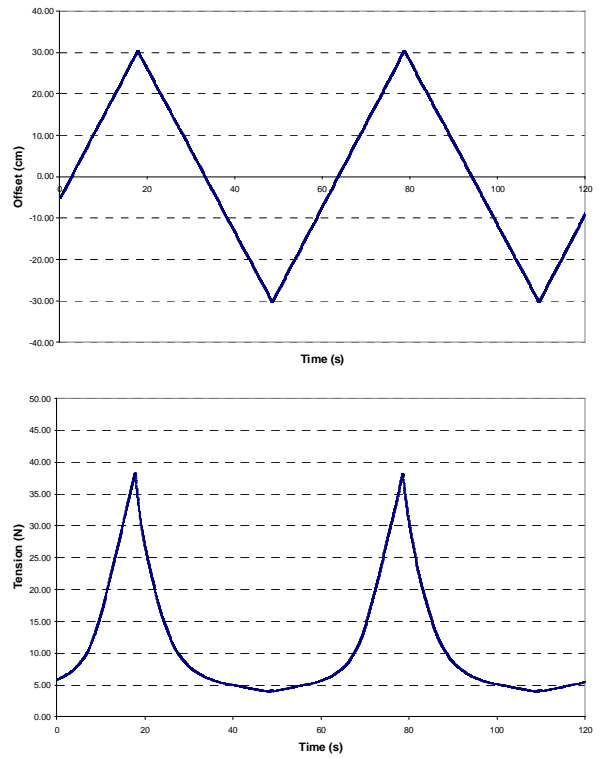


Fig.6 Offset and Static Tension. $\{A_1=0; A_2=0.30\text{m}; f_2=1/60\text{Hz}; U=0\}$

No-drift tests ($A_2=0$) were also performed. In this case, harmonic circular motions with different combinations of amplitude (A_1) and frequency (f_1) were imposed to the top of the model. All these tests were conducted for $R=7.0\text{m}$ (*Neutral* static configuration). Fig.7 presents an excerpt of the time-series of top-end tension measured in the test with $A_1=0.10\text{m}$ and $f_1=0.70\text{Hz}$. In this case $U=0$.

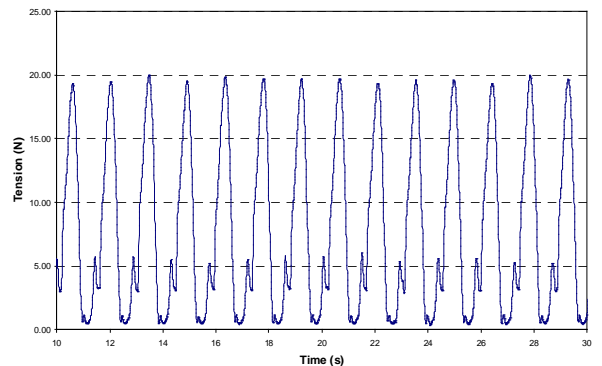


Fig.7 Top-end Tension $\{A_1=0.10\text{m}; f_1=0.70\text{Hz}; A_2=0; U=0\}$

Finally, a series of tests combining 1st and 2nd order motions was performed. Tests comprised all the combinations of amplitudes and frequencies of 1st order ($A_1; f_1$) and drift ($A_2; f_2$) motions, already specified in Table 1. Tension at the top-

¹ The angle is defined with respect to the vertical direction.

end of the model and horizontal excursion were monitored for at least two complete cycles of drift motion. Fig.8 presents the results obtained for $\{A_1=0.05\text{m}; f_1=0.40\text{s}; A_2=0.30\text{m}; f_2=1/80\text{Hz}; U=0\}$.

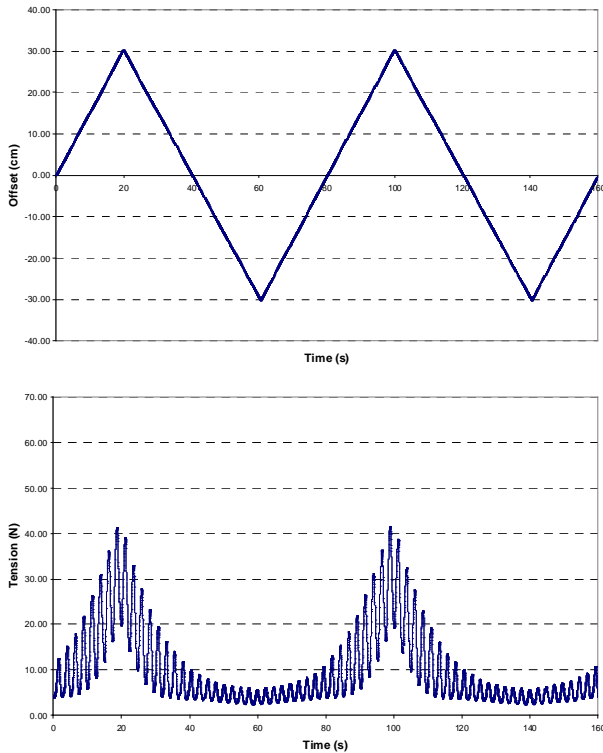


Fig.8 Offset and Static Tension. $\{A_1=0.05\text{m}; f_1=0.40\text{Hz}; A_2=0.30\text{m}; f_2=1/80\text{Hz}; U=0\}$

A case with higher values of dynamic tension amplitude is illustrated by the results in Fig.9, which presents the same drift parameters but higher values of amplitude and frequency of circular motion $\{A_1=0.10\text{m}; f_1=1.00\text{Hz}; A_2=0.30\text{m}; f_2=1/80\text{Hz}; U=0\}$. Compared to the results in Fig.8, it can be seen that the results in Fig.9 present a much higher ratio between dynamic and static tension, as a consequence of the increase in amplitude and frequency of 1st order motion. For offsets around the *Near* position, the tension at the top-end of the model even drops to zero during part of the 1st order cycles, indicating that the top anchor segment slackens for a brief period of time.

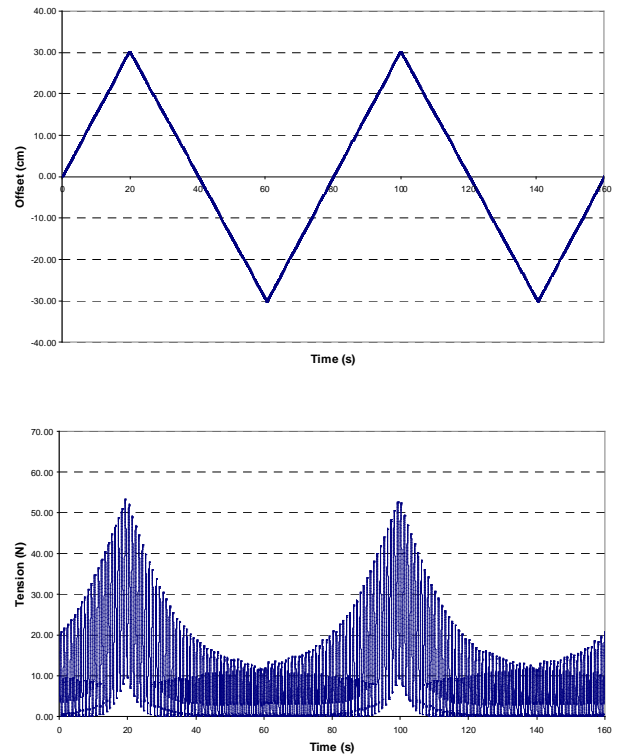


Fig.9 Offset and Static Tension. $\{A_1=0.10\text{m}; f_1=1.00\text{Hz}; A_2=0.30\text{m}; f_2=1/80\text{Hz}; U=0\}$

In such cases, the numerical reproduction of the model dynamics is very demanding in terms of mesh size and, as a consequence, also in terms of computational time. Indeed, one of the goals pursued when defining the parameters for the tests was to obtain results that would request different levels of effort concerning their numerical reproduction. A preliminary discussion regarding this aspect is provided in the next section.

PRELIMINARY NUMERICAL ANALYSIS

Preliminary comparisons between numerical and experimental results were performed at the University of São Paulo. Numerical simulations were performed with the software *Orcaflex*®. Numerical and experimental time-series of tension at the top of the model were compared directly. The main goal of this preliminary analysis was to evaluate the level of difficulty involved in the numerical reproduction of the experimental results obtained in the towing-tank tests. Furthermore, important aspects as numerical stability of the FEM code when dealing with line elongation and the influence of the non-linear structural restoring forces could also be assessed.

For the numerical simulations, a line composed by three segments was created according to the model geometric configuration (see Table 2). Table 4 presents the geometric, structural and hydrodynamic coefficients employed in the

numerical simulations. The chain segment equivalent external diameter and its hydrodynamic coefficients were calculated as suggested in the *Orcaflex*® user manual [8]. All the simulations were performed with an *inner time step* lower than $1/20^{\text{th}}$ of the shortest natural period of the numerical model, as recommended by [8].

Table 4 – Segments Properties for Numerical Simulations

	Chain	Rubber
External Diameter (De)	3.40 mm	12.89 mm
Mass per length (m)	0.068 kg/m	0.173 kg/m
Axial stiffness (EA)	1320 kN	0.759 kN
Bending stiffness (EJ)	0	$7.88\text{E-}3 \text{ Nm}^2$
Normal drag (Cd_N)	1.08	1.00
Axial drag (Cd_A)	0.40	0.10
Normal added mass (Cm_N)	1.00	1.00
Axial added mass (Cm_A)	0.06	0
Normal friction (Cf_N)	0.1%	0.1%
Axial friction (Cf_A)	0.1%	0.1%

Next, some illustrative comparisons between numerical and experimental results will be presented and some important aspects concerning the numerical simulations will be discussed. The first group of tests that was reproduced by means of the FEM code was the one composed by the drift-only tests. Due to the drift motion pattern applied in the tests (half-cycles with constant velocity), the numerical drift motion could not be modeled as a *slow-drift* since *Orcaflex*® assumes those motions to be sinusoidal in time. Therefore, the drift motions had to be considered as successive *steady motions* with constant velocities, each one of them representing one half-cycle of 2nd order motion. Fig.10 presents the comparison between experimental results of the test showed in Fig.6 $\{A_1=0;A_2=0.30\text{m};f_2=1/60\text{Hz};U=0\}$ and the corresponding numerical predictions of offset and tension at the top. The numerical results were simulated for only one cycle of the drift motion (in this case, 60 seconds). Numerical results were obtained with a mesh of 70 elements.

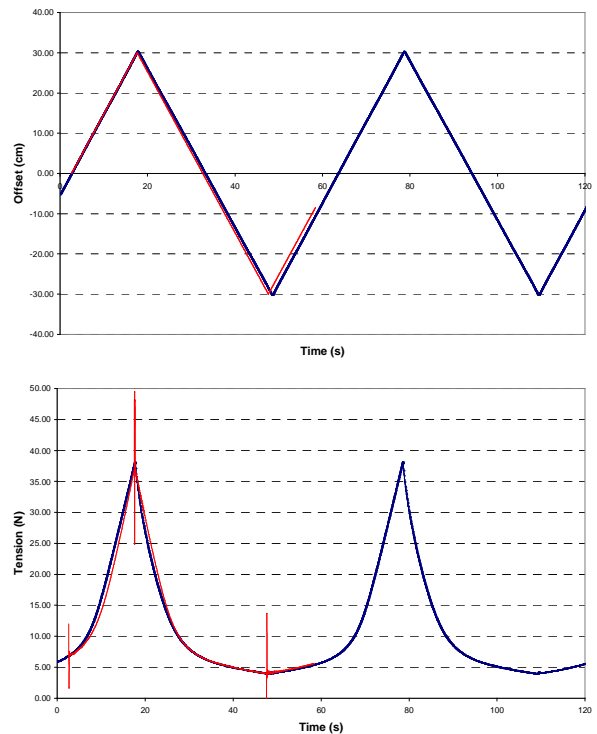


Fig.10 Offset and Static Tension. Experimental (—) and Numerical (—) results. $\{A_1=0;A_2=0.30\text{m};f_2=1/60\text{Hz};U=0\}$

From the results above it can be inferred that the abrupt change in the velocity at the extremities of the horizontal excursion induce sharp tension peaks in the numerical simulations. Such tension peaks are indeed insensitive to the simulation parameters such as mesh size and time-steps. Nevertheless, it was verified that these transitory effects were always almost instantly attenuated and did not represent a hazard concerning the stability of the numerical simulations. It can also be seen that the tension is well captured along the entire drift excursion. The code is able to cope well with line elongation, at least when isolated 2nd order motions are involved.

The 1st order circular motions imposed to the top of the model were emulated numerically by assigning an appropriate RAO (Response Amplitude Operator) to the floating unit and imposing a single harmonic wave (*Airy Wave* in *Orcaflex*®) with the desired frequency of motion. In order to illustrate the overall agreement between the time-series of tension measured in the no-drift tests and the numerical simulations, Fig.11 brings the comparison for the test already presented in Fig.7 $\{A_1=0.10\text{m};f_1=0.70\text{Hz};A_2=0;U=0\}$. In this case, the numerical simulation was performed with a mesh of 210 elements.

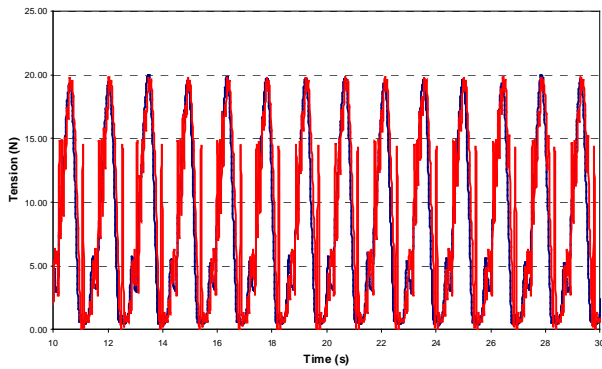


Fig.11 Top-end Tension. Experimental (—) and Numerical (—) results. $\{A_1=0.10\text{m}; f_1=0.70\text{Hz}; A_2=0; U=0\}$

The results above illustrate the agreement observed for the whole set of no-drift tests results. Numerical simulations were able to reproduce the maximum values of tension in all cases tested. As expected, as the tension approaches zero (the line goes slack) some difficulties arise concerning the convergence of the numerical code and some spurious tension peaks can be observed in the time-series close to the instants of minimum tension. Further refining of the numerical mesh can minimize this problem, although simulations become much more time-consuming.

Numerical simulations of the tests that combined 1st and 2nd order motions presented good agreement when compared to experimental results. Difficulties in numerical convergence increase with the amplitude and frequency of the 1st order motion, therefore requiring finer meshes. Fig.12 presents the comparison between the simulated tension variation at the top of the model and experimental results for the test with $\{A_1=0.05\text{m}; f_1=0.40\text{Hz}; A_2=0.30\text{m}; f_2=1/80\text{Hz}; U=0\}$ (test results presented in Fig. 8). This is a somewhat mild case in terms of numerical effort and a mesh with 70 elements was sufficient to guarantee numerical convergence.

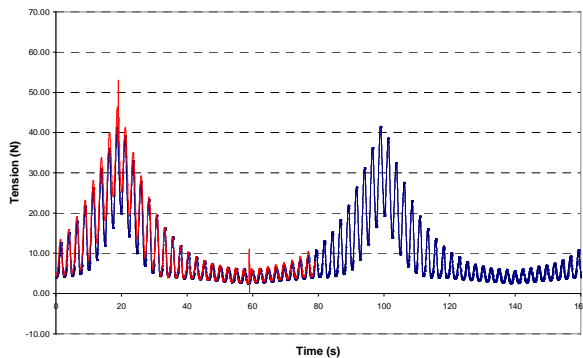


Fig.12 Top-end Tension. Experimental (—) and Numerical (—) results. $\{A_1=0.05\text{m}; f_1=0.40\text{Hz}; A_2=0.30\text{m}; f_2=1/80\text{Hz}; U=0\}$

Reproduction of the results presented in Fig.9 is a much more demanding task due to the higher values of amplitude and frequency of 1st order motion $\{A_1=0.10\text{m}; f_1=1.00\text{Hz};$

$A_2=0.30\text{m}; f_2=1/80\text{Hz}; U=0\}$. Fig.13 compares the results of this test with the simulated time-series of tension obtained with a numerical mesh composed of 260 elements. Convergence becomes particularly difficult as the top-end of the model approaches the *Near* position, due to the decrease in static tension. The time required for the simulation of results presented in Fig.13 was more than 100 times higher than the one required for those in Fig.12 for the same numerical processor.

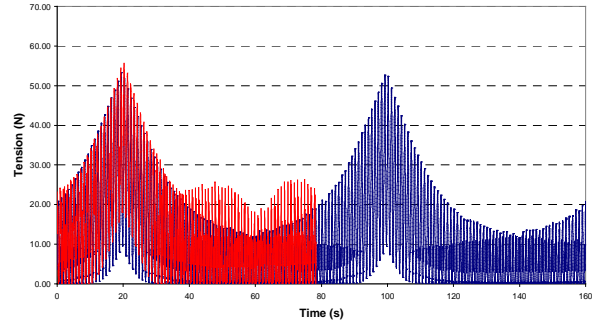


Fig.13 Top-end Tension. Experimental (—) and Numerical (—) results. $\{A_1=0.10\text{m}; f_1=1.00\text{Hz}; A_2=0.30\text{m}; f_2=1/80\text{Hz}; U=0\}$

Results in Figs. 12 and 13 demonstrate that a good quality reproduction of towing tests results can be obtained by means of numerical simulations. In Fig.12, the tension spikes observed around 20 seconds and 60 seconds of simulation result from the abrupt change in the drift motion direction and these transitory effects do not have an effect on the subsequent instants of simulation, a fact that has already been pointed out. In Fig.13, it is possible to see that the discrepancies grow around the *Near* configuration, expressing the numerical difficulties of dealing with situations when the cable slackens (total tension equals zero). Another aspect that must be remarked concerns the somewhat larger discrepancies between simulated and experimental tension around the so-called *Far* position of the top-end. In fact, results in Fig.12 and 13 indicate that the numerical model tends to overestimate slightly the values of maximum tension around 20 seconds of simulation. The probable reason for the somewhat higher discrepancies observed when the line is stretched is the effect of the non-linear behavior of the restoring forces imposed by the rubber hawser (see Fig. 4). Indeed, around the *Far* configuration, elongation of the taut-leg model surpasses 5% and the numerical prediction might be distorted by the assumption of a linear restoring model.

The results presented above illustrate the general agreement observed for the whole set of comparisons performed. Current effects on the static and dynamic tension responses were very well captured by the numerical model, although numerical convergence is slightly more difficult in cases with $U=+0.25\text{m/s}$ as a result of the lower values of static tension.

CONCLUSIONS

A set of experimental results on the dynamic behavior of taut-leg mooring lines was obtained by means of towing-tank tests. The tests involved combined 1st order and drift motions imposed on the top of the model and also current effects. The main goal was to generate a basic experimental paradigm for the validation of numerical codes, as requested by Petrobras. The model was composed by two chain segments in the extremities united by a rubber segment, which was designed to provide the necessary elongation of the model. Test parameters were calibrated in order to provide results that would request very different levels of effort concerning their numerical reproduction.

A preliminary comparison with numerical results was performed at the University of São Paulo, employing the software *Orcaflex*®. The analysis demonstrated that the objectives of the work were successfully reached. It showed that the experimental results can be very well reproduced by means of a validated FEM code. The most demanding tests indeed pose a challenge to the FEM code simulations by requiring fine numerical meshes and, therefore, large computational times in order to guarantee numerical convergence. Current effects clearly exerted an influence on the model dynamics, thus demanding a fair numerical reproduction of the line hydrodynamic properties. Furthermore, the non-linear behavior of the structural restoring forces plays an effective role on the tension as the model is stretched. Dealing with non-linear restoration is an important feature for the numerical codes aimed to predict deep-water taut-leg mooring lines, especially due to the complex structural properties of elements such as polyester or nylon ropes.

A second set of towing-tank tests was performed with a model in catenary configurations. Results are currently being analyzed and will be presented in a future paper.

ACKNOWLEDGMENTS

The authors gratefully acknowledge the support of Petrobras. We are also indebted to the following individuals and their institutions for their invaluable contributions: João V. Sparano (USP), Hélio Correa Jr. (IPT) and Marcelo Ciampolini Neto (IPT).

REFERENCES

- [1] Chaplin, C.R., Del Vecchio, C.J.M., 1992, "Appraisal of Lightweight Moorings for Deep-Water". Proc. of Offshore Technology Conference, Houston, May 1992.
- [2] Fajarra, A.L.C., Simos, A.N., Yamamoto, N., 2003, "Dynamic Compression on Rigid and Flexible Risers. Part I – Experimental Results". Proc. of the 22nd Offshore Mech. and Arctic Eng. Conference, Cancun.
- [3] Kitney, N., Brown, D.T., 2001, "Experimental Investigation of Mooring Line Loading Using Large and Small-Scale Models". Journal of Offshore Mechanics and Arctic Engineering, Vol.123, February.
- [4] Rossi, R.R., 1998, "Recent Developments in the Technical Specification, Design and Installation of Synthetic Mooring Systems: An Update from Brazil". Proc. of the IIR Conf. on Technical Developments in Moorings & Anchors for Deep and Ultra Deep Oil Fields, Aberdeen, Scotland.
- [5] Simos, A.N., Fajarra, A.L.C., Alves, K.H., 2003, "Dynamic Compression on Rigid and Flexible Risers. Part II – Comparison of Theoretical and Experimental Results". Proc. of the 22nd Offshore Mech. and Arctic Eng. Conference, Cancun.
- [6] Simos, A.N., Fajarra, A.L.C., 2004, "Dynamic Tension on Mooring Lines. Comparison of Numerical and Experimental Results". Proc. of the 14th Offshore and Polar Eng. Conf., Toulon, pp.169-174.
- [7] Winkler, M.M., Mackena, H.A., 1995, "The Polyester Taut-Leg Mooring Concept: A Feasible Means for Reducing Deepwater Mooring Cost and Improving Stationkeeping Performance". Proc. of Offshore Technology Conference, Houston, May 1995.
- [8] Orcina Software Ltd. "Visual Orcaflex User Manual", Orcina Ltd, Cumbria, UK.